ORGANOMETALLICS

pubs.acs.org/Organometallics Article

Cyclometalated NHCs Pt(II) Compounds with Chelating P^P and S^S Ligands: From Blue to White Luminescence

Sara Jaime, Lorenzo Arnal, Violeta Sicilia,* and Sara Fuertes*

Cite This: https://dx.doi.org/10.1021/acs.organomet.0c00510 Read Online

ACCESS | Metrics & More | Article Recommendations | Supporting Information

ABSTRACT: Ionic $[Pt(C^C^{*A/B})(P^P)]PF_6$ and neutral $[Pt(C^C^{*A/B})(S^S)]$ complexes were designed and synthesized containing cyclometalated N-heterocyclic carbenes ($C^C^{*A/B}$) and diphosphines (P^P: dpfppe, dcypm) or dithiocarbamates (S^S: dmdtc, pdtc) as chelating ligands. Their structural and spectroscopic properties were investigated and found to be dependent on both cyclometalated ($C^C^{*A/B}$) and ancillary (P^P, S^S) ligands. The photophysical and computational studies for the $[Pt(C^C^{*A/B})(P^P)]^+$complexes disclose the nature of the low-lying electronic transitions to be mainly intraligand charge transfer [ILCT ($C^C^{*A/B}$)] with some contribution of ligand-to-ligand charge transfer (LL'CT) or ligand-to metal charge transfer (LMCT) for the dpfppe or dcypm derivatives, respectively. The blue and cyan emissions of PMMA films doped with the $[Pt(C^C^{*A/B})(P^P)]^+$ complexes exhibited very high quantum yields (QYs) reaching up to ∼90%. However, the low-energy absorptions and emissions of the $[Pt(C^C^{*A/B})(S^S)]$ complexes in solution (rt or 77 K) arise from mixed ILCT $[C^C^{*A/B}]$/MLCT $[d\pi(Pt) \rightarrow \pi^*(C^C^{*A/B})]$ excited states, showing no change with the different S^S ligands. In solid-state and in doped films, these dithiocarbamate complexes, excluding **8B**, display dual emissions with the high-energy vibronic band (^{3}ILCT /^{3}MLCT) appearing together with an additional low-energy structureless band. The latter is attributed to $^3\pi\pi^*$ transitions originated from π-stacked aggregates, as reported in the X-ray structure of **7A**. Thus, white light emissions can be obtained with photo- and colorimetric values lying inside the stipulated limits for general lighting applications; yet, they display low QY.

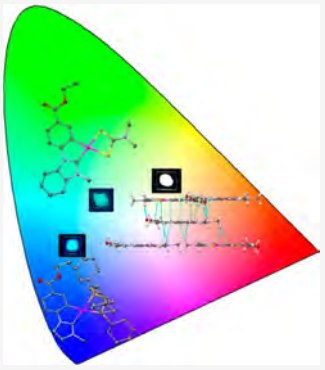

INTRODUCTION

Generation of high quality white light is still one of the major challenging research areas in the field of luminescent materials,[1−3] especially because it requires extremely efficient phosphors to emit light across the whole visible spectral region. Most of the devices reported to date are based on two different approaches: down conversion by phosphors (yellow/orange phosphor pumped with a blue led) and combinations of different phosphors (red/blue/green or blue/orange) deposited on a single blended emitting layer or on a multilayered stacked structure. However, high current density, color aging, fabrication costs, and energy transfer between emitters are some of the encountered problems derived from these device architectures.[3,4] On the contrary, single-emitter based white organic light-emitting diodes (WOLEDs) should be expected to address these weaknesses, thus giving rise to simple fabrication processes and white light of higher quality.[5−23]

Lately, to tackle this challenge, square planar platinum(II) complexes with elevated luminescent efficiencies have been moved to the forefront as excellent candidates to be used on single-doped WOLEDs.[13−23] This class of phosphorescent complexes has proven the ability to emit blue and orange-red lights. The former comes from ^{3}IL/^{3}MLCT excited states characteristics of isolated Pt molecules, whereas the latter arises from ^{3}MMLCT and/or $^3\pi\pi^*$ excited states generated by ground- and excited-state interactions between the monomers which are permitted by the square-planar geometry of the Pt(II) center. Consequently, by adjusting the doping concentration of the Pt phosphor in these devices, well-balanced white light can be successfully obtained from the combination of the monomer and excimer/aggregate emissions. This strategy has been commonly employed; however, the color rendering index (CRI) of the output light is still below 80.[15−23] Also, highly efficient blue emitting Pt compounds are still scarce, and some device architectures use OLEDs components such as 4,4′-bis-[*N*-(1-naphthyl)-*N*-phenylamino]biphenyl (NPB) or 4,4′-bis(9-ethyl-3-carbazovinylene)-1,10-biphenyl (BCzVBi) as both blue emitters and transport layer materials.[24−26]

A rational approach for the design of efficient blue emitters is the incorporation of cyclometalated N-heterocyclic carbenes (C^C*), which may surpass the high ligand field splitting capacity of the C^N-ligands (cyclometalated imines), since they present two C-σ bonds. Another consequence of the

Received: July 28, 2020

https://dx.doi.org/10.1021/acs.organomet.0c00510
Organometallics XXXX, XXX, XXX−XXX

presence of strong carbon−metal bonds is the robustness and/or stability of the NHC complexes which may provide long-lasting functional materials.[27−32] Additionally, the use of C^C* bidentate ligands has the advantages of modulating the emission color and improving their quantum efficiencies, both of which can be accomplished by selecting the appropriate ancillary ligands when designing the square-planar Pt(II) emitter. Rigid scaffolds with chelating coordination and strong donor atoms are desired structural features to minimize excited-state structural deformations and improve emission quantum yields,[13,17−22,33,34] due to their great influence on the radiation-less decay rate constant. These structural distortions enhance the electron-vibrational coupling of the excited and the ground states and, as a result, promote nonradiative decays.[35]

Given the great interest in stable and efficient luminescent compounds and our previous results of bright-blue emitters using cyclometalated NHC complexes of Pt(II),[36−40] we decided to investigate new Pt(C^C*) systems with different chelating ancillary ligands that present varied steric and electronic properties. Thus, we prepared a new NHC cycloplatinated compound [Pt(C^C*^{A})ClMeCN] (HC^C*^{A}-κC*^{A} = 1-(4-(ethoxycarbonyl)phenyl)-3-methyl-1*H*-benzimidazol-2-ylidene, **4A**) following our stepwise procedure. Then, by using this and [{Pt(μ-Cl)(C^C*^{B})}$_2$] (HC^C*^{B}-κC*^{B} = 1-(4-(ethoxycarbonyl)phenyl)-3-methyl-1*H*-imidazol-2-ylidene, **4B**),[41] new cationic, [Pt(C^C*$^{A/B}$)(P^P)]$^{+}$, and neutral, [Pt(C^C*$^{A/B}$)(S^S)], complexes of Pt(II) have been prepared, where P^P is bis(dipentafluorophenylphosphino)ethane (dpfppe **5A**, **5B**) and bis(dicyclohexylphosphino)methane (dcypm **6A**, **6B**) and S^S is dimethyldithiocarbamate (dmdtc^{-} **7A**, **7B**) or pyrrolidinedithiocarbamate (pdtc^{-} **8A**, **8B**), both acting as chelate ligands. The photophysical properties of all complexes were deeply examined and correlated to the X-ray structures and DFT calculations.

RESULTS AND DISCUSSION

Step-by-Step Procedure of C^C*-Cyclometalated N-Heterocyclic Pt (II) Compound. The synthesis of the new ligand HC^C*^{A} and its subsequent cyclometalation to a Pt (II) center was achieved following our reported method for related compounds (Scheme 1, Experimental Section, and Figures S1−S6 in the Supporting Information).[41−44] Ethyl-4-bromobenzoate was coupled with benzimidazole in DMSO at 130 °C using Cu_2O and K_2CO_3 in the presence of 4 Å molecular sieves, under Ar atmosphere. After 24 h, the work up obtained **1A** as a white solid (Scheme S1, path a). Then, **1A** was reacted with CH_3I in refluxing THF for 24 h (scheme S1, path b) under Ar conditions to give **2A** as a white solid. The synthesis of this new benzimidazolium salt, 1-(4-(ethoxycarbonyl)-phenyl)-3-methyl-1*H*-benzimidazolium iodide (**2A**), required reaction conditions more severe and gave a lower yield than those for the analogous 1-(4-(ethoxycarbonyl)phenyl)-3-methyl-1*H*-imidazolium iodide,[41] most likely due to the conjugation effect of the benzene ring fused to the imidazole fragment. The activation of the C1−H1 bond and formation of the corresponding silver carbene was achieved by reaction of **2A** with Ag_2O in anhydrous dichloromethane and Ar atmosphere in the dark. After 3h at rt, [{Pt(μ-Cl)(η^3-2-Me-C_3H_4)}$_2$] was added to the reaction and allowed to react for 12 h yielding **3A** (Scheme 1, path a).

The cyclometalation of the N-heterocyclic carbene was achieved by refluxing **3A** in 2-methoxyethanol. The subsequent recrystallization of the resulting gray solid, most likely [{Pt(μ-Cl)(C^C*^{A})}$_2$], in refluxing acetonitrile gave **4A**, as a mixture of two isomers *cis*-(C*, Cl) and *trans*-(C*, Cl) (Scheme 1, paths b and c). The chloro-bridge splitting can give a mixture of *cis*- and *trans*-(C*,Cl) isomers,[43] which are related with the degree of transphobia (T) of pairs of *trans* ligands.[45,46] The ^{1}H NMR spectrum of **4A** in DMSO-d_6 (Figure S6) showed the absence of the allyl group, the presence of a molecule of free acetonitrile, and two sets of resonances corresponding to the two geometrical isomers obtained from the displacement of the MeCN by coordination of the deuterated solvent.

C^C*-Cyclometalated Compounds of Pt(II) with Chelating P^P and S^S Ligands: Synthesis and Characterization. Compounds [Pt(C^C*$^{A/B}$)(P^P)]PF$_6$ (P^P = dpfppe, C^C*^{A} **5A**, C^C*^{B} **5B**; dcypm, C^C*^{A} **6A**, C^C*^{B} **6B**) were prepared by treatment of a suspension of the corresponding starting compounds, *cis*-, *trans*-(C*,Cl) [Pt(C^C*^{A})ClMeCN] (**4A**) or [{Pt(μ-Cl)(C^C*^{B})}$_2$] (**4B**),[41] in acetone at rt, with the diphosphine and KPF_6 (Scheme 2 and Experimental Section). After work up, these compounds were obtained as pure solids and then completely characterized (Experimental Section and Figures S7−S34). The structural information harvested from NMR spectra sustains the proposed structure for these compounds.

Scheme 1. Stepwise Synthesis

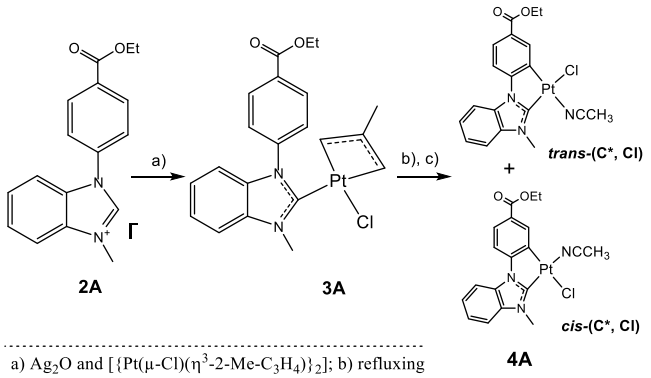

a) Ag_2O and [{Pt(μ-Cl)(η^3-2-Me-C_3H_4)}$_2$]; b) refluxing 2-MeOEtOH; c) recrystallization in refluxing MeCN

Scheme 2. Chemical Structure of the Complexes and Atom Numbering for NMR Purposes

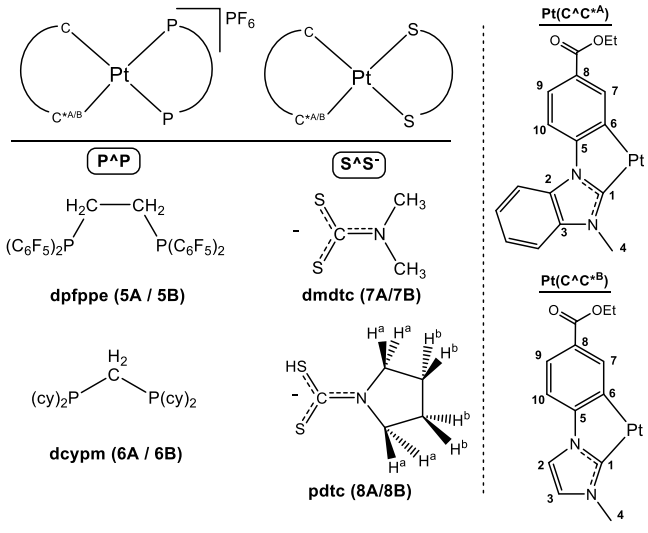

https://dx.doi.org/10.1021/acs.organomet.0c00510
Organometallics XXXX, XXX, XXX−XXX

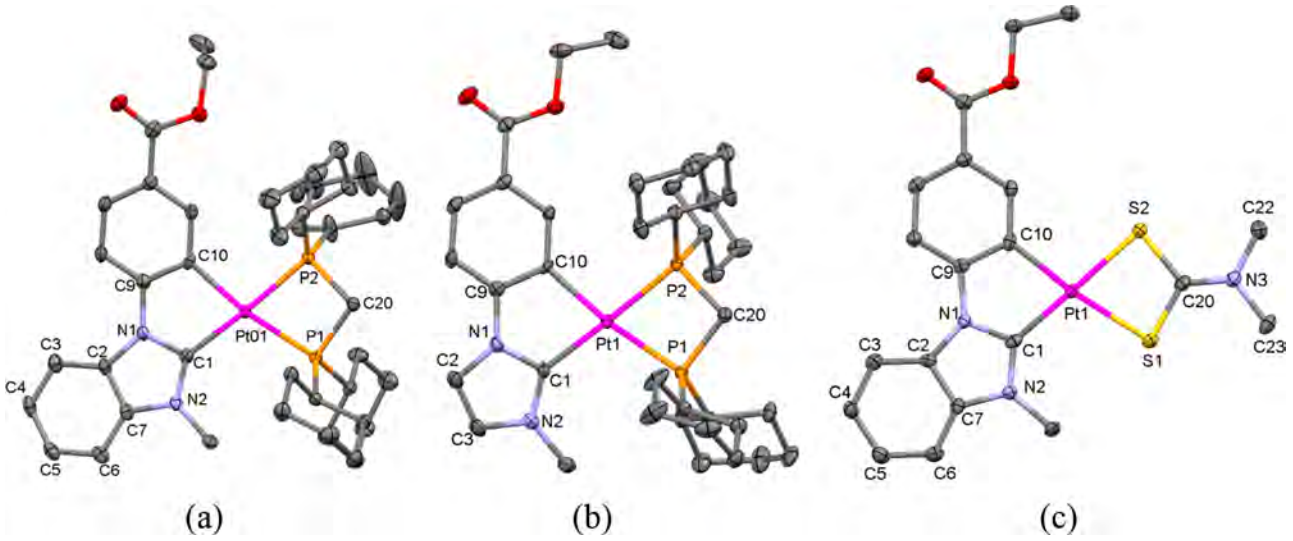

Figure 1. Molecular structures of **6A** (a), **6B** (b), and **7A** (c).Thermal ellipsoids are drawn at the 50% probability level. Hydrogen atoms, solvent, and PF_6 molecules have been omitted.

In their $^{31}P\{^1H\}$ NMR spectra, the two inequivalent P atoms of the dpfppe ligand in **5A** and **5B** gave two broad signals, due to the coupling with the fluorine atoms (Figure S33). However, those of the dcypm in **6A** and **6B**, which are in close proximity, give rise to two doublets, with a $^2J_{P,P}$. values of ca. 36 Hz. Every signal appears flanked by the corresponding ^{195}Pt satellites with $^1J_{Pt,P}$ values of 2800−2200 Hz or 1800−1400 Hz for the P atoms located in the *trans* position to the carbene (C*) or the aromatic C atom (C_{Ar}), respectively, in agreement with the smaller *trans* influence of C* compared to that of C_{Ar}.[43] As expected, for each of the four complexes (**5A**/**B**, **6A**/**B**), the $^{195}Pt\{^1H\}$ NMR spectrum shows a doublet of doublets due to the coupling of the Pt center to two inequivalent P atoms (Figure S34). It is worth noting the downfield shift of the ^{195}Pt signal in dcypm (**6A**, **6B**) derivatives compared to those of the dpfppe ones (**5A**, **5B**), which can be attributed to the great strain in the four-membered ring (Pt−P−C-P).[47,48] Also, considering the $\delta^{31}P$, $\delta^{195}Pt$, and J_{Pt-P} values, the C^C*^{A} fragment seems to withdraw more electron density from the Pt center than the C^C*^{B} moiety, probably caused by the electron withdrawing (EW) effect of the benzene ring fused to the imidazole fragment. This is in agreement with the electron density distribution obtained from the natural bond orbital (NBO) analysis on the platinum centers, −0.076 (**6A**) and −0.092 (**6B**).

In order to compare the effects of the ancillary ligand on the photophysical properties, we expanded the work using chelate ligands with less steric hindrance and different electronic properties. Thus, we prepared the neutral compounds [Pt(C^C*$^{A/B}$)(S^S)] (S^S = dmdtc$^-$, C^C*^{A} **7A**, C^C*^{B} **7B**; pdtc$^-$, C^C*^{A} **8A**, C^C*^{B} **8B**) by reaction of the "in situ" generated species, [Pt(C^C*$^{A/B}$)(NCMe)$_2$]PF_6, with equimolecular amounts of NH_4(pdtc) or Na(dmdtc) in MeOH (Scheme 2 and Experimental Section for details). All four compounds **7A**/**B** and **8A**/**B** were obtained as air-stable solids and fully characterized. Their IR spectra exhibit intense absorptions at ca. 1540 cm^{-1} due to the C−N stretching vibration in the dithiocarbamate groups. These values are in-between those recorded for single C−N (1360−1250 cm^{-1}) and double C═N (1690−1640 cm^{-1}) bonds, revealing a great degree of C−N double bounding character.[49] Also, the υ(C−S) and υ(Pt−S) absorptions indicate that the dithiocarbamates are coordinating as chelate ligands.[49−52] The ^1H and $^{13}C\{^1H\}$ NMR spectra in CD_2Cl_2 solution at rt display the expected signals for the ligand C^C* and the dithiocarbamate ligands (Figures S35−S54). Following the same trend observed for the P^P derivatives, the ^{195}Pt signals of the C^C*^{A} complexes appear more deshielded than those for the C^C*^{B} counterparts (Figure S55).

The X-ray study of **6A**, **6B**, and **7A** (Figures 1, S56, and S57 and Table 1) confirmed their molecular structures showing a

Table 1. Selected Bond Lengths (Å) and Angles (deg) for 6A, 6B, and 7A

	6A (X = P)	**6B** (X = P; Pt1/Pt1A)[a]	**7A** (X = S)
Pt(1)−C(1)	2.043(3)	2.043(6)/2.046(6)	1.972(3)
Pt(1)−C(10)	2.058(3)	2.061(5)/2.061(6)	2.027(3)
Pt(1)−X(1)	2.3580(9)	2.3293(15)/2.3385(16)	2.3895(7)
Pt(1)−X(2)	2.3063(9)	2.2931(16)/2.2835(16)	2.3462(8)
C(1)−Pt(1)−C(10)	78.47(13)	79.0(2)/78.9(3)	79.71(12)
C(1)−Pt(1)−X(1)	110.17(9)	107.75(18)/109.71(18)	106.30(9)
X(1)−Pt(1)−X(2)	72.16(3)	73.19(5)/72.82(6)	74.19(3)
C(10)−Pt(1)−X(2)	98.97(10)	99.32(18)/98.46(19)	99.81(9)
plane1−plane2	3.43(7)	10.71(7)/5.79(7)	0.98(7)

[a]The asymmetric unit of **6B** contains two molecules (Pt1 and Pt1A). Plane1 = [Pt, C1, C10, C9, N1], and plane2 = [Pt, C1, C10, X1, X2].

really distorted square-planar coordination environment for the metal with C(1)−Pt−C(10) and X(1)−Pt−X(2) (X = P for **6A** and **6B**, S for **7A**) bite angles of 79°−73°. Regarding the "Pt(C^C*$^{A/B}$)" moiety, the Pt−C bond parameters are similar to those of reported platinacycles with N-heterocyclic carbenes,[28,29,36,38,40−44] and the five-membered platinacycle and the Pt coordination plane result almost coplanar (Table1).

In **6A** and **6B**, the Pt−P1 bond lengths are longer than those of the Pt−P2 ones, in line with the C_{Ar} (C10) atom having a higher *trans* influence than the carbenic one (C1).[43] The P−Pt−P bite angles are significantly smaller than 90° (~73°), due to the great strain exerted by the four-membered chelate ring. In **7A**, the narrow bite angle S−Pt−S and Pt−S and C−S bond

https://dx.doi.org/10.1021/acs.organomet.0c00510
Organometallics XXXX, XXX, XXX−XXX

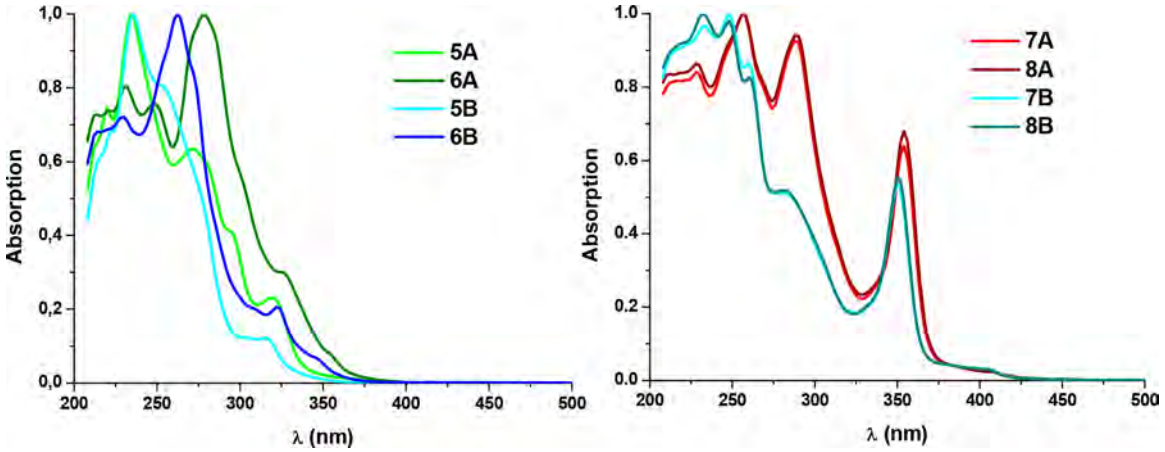

Figure 2. Normalized UV−vis spectra in CH_2Cl_2 solution (5×10^{-5} M).

distances are comparable to those from other dithiocarbamate complexes of Pt(II).[51,52]

In their crystal structure packings, there are no Pt−Pt contacts. However, the molecules organize themselves in head-to-tail pairs through offset $\pi\cdots\pi$ intermolecular contacts (3.30 Å) among the benzimidazole rings in **6A** and almost overlapped $\pi\cdots\pi$ interactions (3.38−3.34 Å) between the C^C*^{A} moieties in **7A** (Figure S57a,b). Additionally, these head-to-tail pairs in **7A** self-assembled each other by the assistance of secondary intermolecular contacts (C−H···O, C−H···π, and $\pi\cdots\pi$), in such a way that the dithiocarbamate ligands from one head-to-tail unit are interacting with the C^C*^{A} fragments belonging to the adjacent pairs (Figure S57c). Also, in **6A**, the PF_6^- anions are acting as bridges between these head-to-tail pairs through weak C−H···F contacts (d C···F = 3.09−3.35 Å; d H···F = 2.61−2.85 Å, Figure S57a).

Photophysical Properties and Theoretical Calculations. *Absorption Spectra.* The UV−vis spectra of all compounds in different solvents at 5×10^{-5} M are illustrated in Figures 2 and S58, and their data are listed in Table S2. They exhibit intense absorptions at $\lambda \leq 300$ nm which are usually attributed to intraligand (^{1}IL) transitions of the C^C* ligand. The diphosphine complexes show also bands at around 320 nm with less intense absorptions at ca. 350 nm that do not show any significant solvatochromism (Figure S58, left), yet sensitive to both the C^C* and the ancillary ligands. When comparing compounds with the same N-heterocyclic carbene (C^C*) but different P^P (**5A** vs **6A** or **5B** vs **6B**), the absorptions of the dpfppe derivatives appear shifted to higher energies with respect to those of the dcypm ones (i.e., λ = 316 nm, **5B**; 322 nm **6B**).

Likewise, when relating compounds with the same P^P ligand but different C^C* (**A** vs **B**), it can be observed that the absorptions of the **A** compounds appear shifted to lower energies in relation to those of the **B** ones (λ = 320 nm, **5A**; 316 nm, **5B**). Thus, both C^C* and P^P ligands seem to be involved in the lowest-energy spin-allowed transitions. This same trend (red-shift of **A** vs **B**) is also observed in the S^S derivatives. They display strong absorptions at around 350 nm with weak low-lying bands at ca. 400 nm that do not change with the dithiocarbamate ligands (Figure 2, right).

To determine if these bands at 400 nm were associated with intermolecular transitions, the absorption spectra of **7B** was registered in CH_2Cl_2 at concentrations ranging from 10^{-3} to 10^{-6} M. As shown in Figure S59, the absorption at 400 nm obeys Beer's law, suggesting that they are due to transitions in the molecular species and no significant aggregation occurs within this concentration range.

Theoretical calculations of compounds [Pt(C^C*$^{A/B}$)(P^P)]PF_6 (**5A**, **6A**, **6B**) and [Pt(C^C*^{A})(dmdtc)] (**7A**) have been performed to help with the correct assignments for the experimental UV−vis absorptions (Tables S3 and S4 and Figure S60). TD-DFT vertical excitation energies were computed at the ground-state geometry in CH_2Cl_2 solution and point out that the HOMO → LUMO transition is the only contribution to the singlet electronic $S_0 \rightarrow S_1$ transition (Table S4). Therefore, since the TD-DFT vertical excitation energies fit well with the lowest-energy absorptions represented in the experimental spectra (Figure S60), their assigments can be carried out by analyzing the compositions of the frontier molecular orbitals (FOs: HOMO−LUMO). By comparing compounds which only differ in the C^C* (**6A** and **6B**), it can be observed that the nature and composition of the FOs are very similar (Table S3). Regarding the FO compositions of the diphosphine derivatives (**5A**, **6A**, and **6B**), their HOMOs are rather similar and are mainly centered on the C^C* ligand (74−90%) and the Pt center (10−24%), while the LUMOs show a higher participation of the P^P ligands and minor contribution of the C^C* fragments, especially for **5A** (14% Pt, 46% C^C*, 40% P^P). Thus, if we compare it with that of **6A** (24% Pt, 63% C^C*, 13% P^P), it can concluded that the low-energy absorption for the fluorophenyl diphosphine derivatives (**5A**/**B**) is attributed to mixed ligand-to-ligand charge transfer (LL'CT) [π(C^C*) → π*(P^P)] and ILCT [π(C^C*) → π*(C^C*)] transitions, whereas that for the cyclohexyl diphosphine ones (**6A**/**B**) is mostly assigned to ILCT [π(C^C*) → π*(C^C*)] transitions with some LL'CT [π(C^C*) → π*(P^P)] and LMCT [π(C^C*) → dπ*(Pt)] character. On the other hand, considering that the change of the dithiocarbamate ligand (dmdtc vs pdtc) does not have any influence on the UV−vis absorptions (Figure 2, right), only complex **7A** was studied. As can be observed in Table S3 and Figure S60d, the HOMO greatly differs from those of the P^P derivatives (**5A** and **6A**) and is distributed over the Pt center, the C^C* and S^S ligands with proportions of ca. 30% each; however, the LUMO is mainly localized on the C^C* (66%) fragment with small contributions of the Pt (18%) and S^S (16%) moieties. Hence, the low-energy absorption in **7A**

https://dx.doi.org/10.1021/acs.organomet.0c00510
Organometallics XXXX, XXX, XXX−XXX

seems to arise from combined transitions MLCT [$d\pi$(Pt) → π^*(C^C*)]/L'LCT [π(S^S) → π^*(C^C*)].[51]

Emission Spectra. Emission data of all compounds in different media are listed in Table 2, and relevant spectra are represented in Figures 3−5 and S61−S66.

Table 2. Emission Data

compd	media (T/K)	λ_{ex} (nm)	λ_{em} (nm)	τ (μs)[c]	ϕ (%)
5A	2-MeTHF[a,b] (77)	320	453$_{max}$, 483, 517, 552$_{sh}$	32.8	
	5 wt % film	330	470, 493$_{max}$, 522$_{sh}$	22.5	83
	solid (298)	350	474$_{sh}$, 498$_{max}$, 530$_{sh}$	4.5	6
5B	2-MeTHF[a,b] (77)	315	442$_{max}$, 472, 504, 548	36.3	
		450	550[d]		
	5 wt % film	320	452, 478$_{max}$, 508$_{sh}$	24.6	78
		380	452, 478, 520[d]		
	solid (298)	340	457$_{sh}$, 481$_{max}$, 510	4.7	7
		380	456$_{sh}$, 483$_{sh}$, 530$_{max}$	0.8	9
6A	2-MeTHF[a,b] (77)	350	461$_{max}$, 491, 523, 560sh	20.1	
	5 wt % film	330	471, 496$_{max}$, 529$_{sh}$	14.9	89
	solid (298)	370	473, 499$_{max}$, 530	14.4	50
6B	2-MeTHF[a,b] (77)	345	453$_{max}$, 484, 516, 554$_{sh}$	20.6	
	5 wt % film	320	457, 487$_{max}$, 516$_{sh}$	15.7	88
	solid (298)	360	455, 482$_{max}$, 510	13.1	57
7A	2-MeTHF[a] (77)	355	460$_{max}$, 491, 525	5.8	
	2 wt % film	350−400	476$_{max}$, 505, 542sh, 600	3.4 [476] 0.7 [600]	12
	40 wt % film	350−400	476$_{max}$, 505, 542sh, 600	3.7 [476] 0.7 [600]	10
	solid (298)	400	477, 507$_{max}$, 542, 600	5.3 [477] 0.9 [600]	4 2
7B	2-MeTHF[a] (77)	352	458$_{max}$, 489, 522	6.2	
	2 wt % film	350	463$_{max}$, 493, 520$_{sh}$	4.7	12
		400	464, 494, 570$_{max}$	1.3	7
	40 wt % film	350	463$_{max}$, 495, 570	4.1	8
		400	464, 494, 570$_{max}$	0.8	6
	solid (298)	400	467, 494$_{max}$, 620	5.8 [467] 1.5 [620]	8
8A	2-MeTHF[a] (77)	355	460$_{max}$, 491, 526	5.6	
	solid (298)	400	468, 497, 600$_{max}$	1.1	6
8B	2-MeTHF[a] (77)	352	458$_{max}$, 489, 522	5.9	
	solid (298)	400	466$_{max}$, 494, 533$_{sh}$	4.8	5

[a]10^{-5} M. [b]10^{-3} M. [c]Measured at λ_{max} unless stated otherwise. [d]Too weak to record ϕ and τ.

[Pt(C^C)(P^P)]PF_6 Complexes.* Compounds **5A**/**B** and **6A**/**B** exhibit strongly structured emission bands with maxima in the blue region in glassy 2-MeTHF, in poly(methyl methacrylate) (PMMA) films (5 wt % doped) and in solid state (for an example, see Figure S61). As shown in Figure 3 left, the complexes containing the C^C*^{A} group display emissions shifted to lower energies with respect to those containing the C^C*^{B} one, and the dpfppe derivatives display emissions shifted to higher energies when compared to those of the dcypm ones, following the trend observed for the lowest-energy absorption bands. Emission decays fitted to one component with those recorded for the dpfppe derivatives (ca. 33 μs) being slightly longer than those obtained for the dcypm counterparts (ca. 20 μs).

The geometries of S_0 and T_1 were optimized and the emission energies calculated as ΔE_{T1-S0} (463, 477, and 460 nm, **5A**, **6A**, and **6B**, respectively) are in close agreement with the experimental values registered for 2-MeTHF (10^{-5} M, 77 K) (453, 461, and 453 nm for **5A**, **6A**, and **6B**, respectively). As depicted in Figure 3 right, the spin-density distributions are essentially centered on the C^C* ligand with a minor participation of the Pt center. They result to be very similar to the electronic distributions in the HOMOs (see Figure S60), pointing to a ^{3}IL [C^C*] nature of the emission for all P^P complexes. The slightly higher contribution of the metal orbitals to the emissive state in the dcypm derivatives (**6A** and **6B**) leads to shorter emission decays compared to those of the dpfppe ones (**5A** and **5B**). The higher intensity of the lowest-energy band (ca. 550 nm) in **5B** (cyan line in Figure 3) when compared to the others has been studied in detail. In glassy solutions of 2-MeTHF, upon excitation at λ_{ex} = 450 nm, the emission profile changes, whereby a weaker and structureless band appears at λ_{max} = 550 nm either at low (10^{-5} M) or high (10^{-3} M) concentration (Figure S62). Likewise, when exciting at λ > 380 nm in 5 wt % PMMA film or powder (Figure S63), **5B** shows an additional low-energy (LE) band at ca. 530 nm fitting a rather short lifetime decay (0.8 μs). In light of this, we also registered the emission spectra of 2 and 40 wt % PMMA films (Figure S63, right). The intensity of the LE band for the 2 wt % film is weaker in relation to those for 5 and 40 wt % when exciting at 380 nm, and it is tentatively attributed to $^3\pi\pi^*$ transitions.

Quantum yield (QY) measurements were carried out on 5 wt % doped PMMA films and powder samples exposed to the air atmosphere. The results in PMMA reveal that all complexes exhibit very high QY values in the blue−cyan spectral region (~80% for **5A** and **5B** and ~90% for **6A** and **6B**), whereas in powder, the dpfppe derivatives (**5A**/**B**) displayed rather low efficiencies (~ 6%) in relation to those recorded for the dcypm counterparts (50%, **6A**; 57%, **6B**).

If we compare the powder QY of **5B** (7%) and **6B** (57%), with [Pt(C^C*^{B})(P^P)]PF_6 (P^P = dppm, dppe, dppbz) [QY = 10−40%],[38] having the same cyclometalated carbene (C^C*^{B}) but different P^P ligand, it can be observed the great influence of the chelating diphosphine. Also, compound **6B** proved to be among or even better than the best blue Pt(II) emitters whether in solid state or doped film.[28,34,36−40,53−57] Nonetheless, the CIE coordinates (0.17, 0.30) slightly deviate from the desired ones for deep blue emitters (0.15, 0.22), see Figure 4.

[Pt(C^C)(S^S)] Complexes.* In glassy 2-MeTHF (10^{-5} M, 77 K), the emission spectra of the compounds **7A**/**B** and **8A**/**B** display highly structured bands with vibronic spacings of ca.

https://dx.doi.org/10.1021/acs.organomet.0c00510
Organometallics XXXX, XXX, XXX−XXX

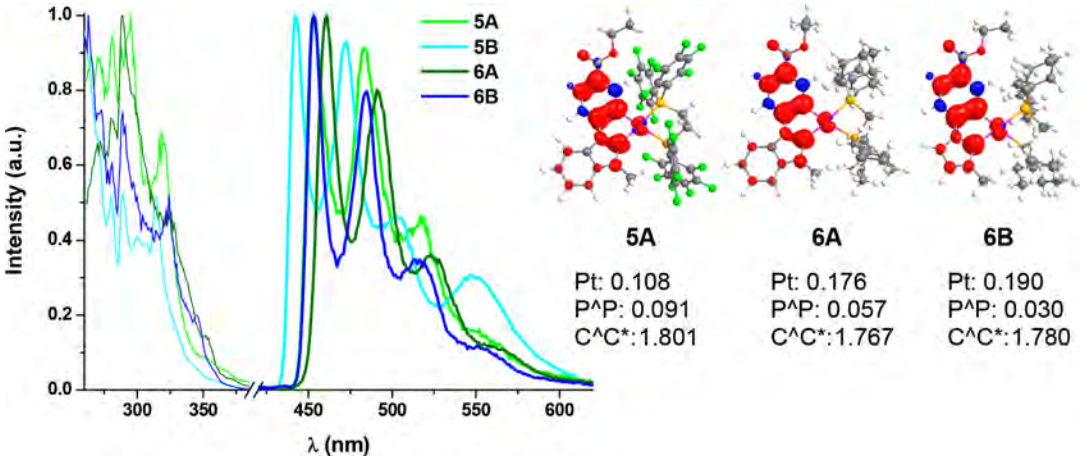

Figure 3. Left: normalized excitation (−) and emission (——) spectra in 2-MeTHF (10^{-5} M, 77K). Right: Spin-density distribution plots (isovalue: 0.002) for the T_1 state.

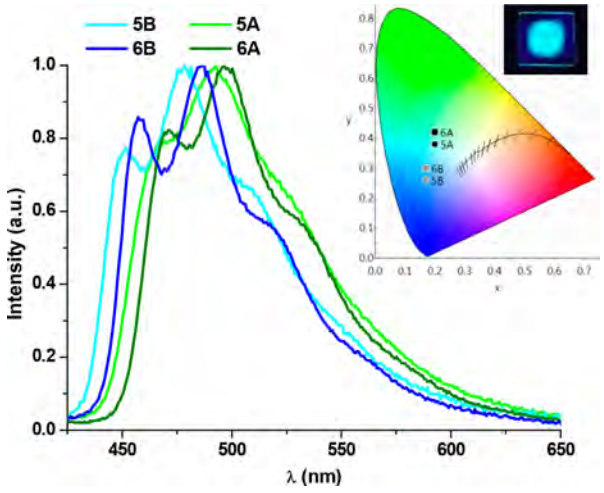

Figure 4. Normalized emission spectra in 5 wt % PMMA films. Inset: CIE 1931 chromaticity diagram; picture of **6B** taken under UV (365 nm) light.

1300 cm^{-1}, corresponding to the IR stretches of the cyclometalated C^C* ligand and lifetime decays of ∼6 μs. As depicted in Figure S64, the excitation and emission profiles barely change with the nature of the ancillary (S^S) or the cyclometalated (C^C*) ligands, just 2 nm shift between A and B counterparts. Bearing in mind this and the analysis of T_1 spin-density distribution (Figure S64) of **7A** versus the electronic distribution in the HOMO (Figure S60), these emissions are reasonably assigned to mixed ^{3}ILCT [C^C*]/^{3}MLCT [dπ(Pt) → π*(C^C*)] excited states, alike related cycloplatinated compounds with chelating dithiocarbamates.[51,58] The higher participation of the platinum center to the excited states is reflected on the decrease of the lifetime values compared with those for the P^P derivatives. In solid state, the emission spectra of all four complexes present a vibronic band at high energy (E_{em}(0−0) ∼ 460 nm) together with a broad structureless band with maxima at about 600 nm (LE band), except for **8B** that only exhibits the high energy (HE) band (Figure S65). The emission profiles do not depend on the excitation wavelength and the lifetime decays of the HE and LE bands fit to one component, ca. 5 and 1 μs, respectively. Thus, keeping all this in mind and the π-stacked packings reported in the X-ray structure of **7A** (Figure S57), the LE band can be attributed to $^3ππ^*$ transitions due to the formation of aggregates as a result of π−π interactions among C^C* groups from adjacent molecules.[38,40,42] Considering the analogous emission features (vibronic structure, energy and lifetime) of the HE band with those obtained in 2-MeTHF (10^{-5} M, 77 K), it seems reasonable to assume the same emissive origin, ^{3}ILCT/^{3}MLCT for them.

Given the solid-state emissive behavior of the S^S derivatives, we measured their quantum efficiencies on powder samples and on doped PMMA films, at two different concentrations (2 and 40 wt %; only for **7A** and **7B** due to solubility issues). The spectra of **7A** in PMMA films show the same emission profiles regardless of the doping concentration or excitation wavelength (Figure S66). On the contrary, the emission of **7B** depends on both the doping concentration and also the $λ_{ex}$ (Figure 5). Thus, if a 2 wt % PMMA film is excited with $λ$ = 350 nm, only the HE band is detected, but if $λ_{ex}$ = 400 nm, the spectrum shows the two contributions, the HE and LE. However, when increasing the doping concentration up to 40 wt %, both emissions can be registered whether exciting at short (350 nm) or longer (400 nm) wavelengths.

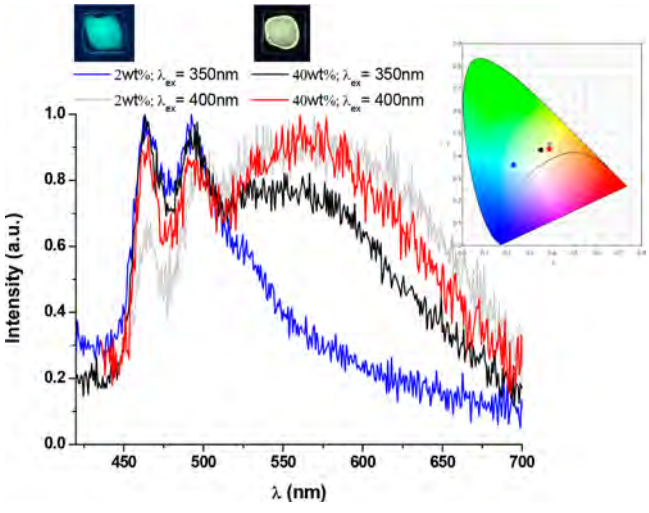

Figure 5. Normalized emission spectra of **7B** in doped films. Pictures of 2 wt % (left) and 40 wt % (right) films taken under UV light (365 nm). Inset: CIE 1931 chromatic diagram.

https://dx.doi.org/10.1021/acs.organomet.0c00510
Organometallics XXXX, XXX, XXX−XXX

The quantum yields of **7A** and **7B** in doped films range between 7 and 12% and those recorded in solid state around 4−8%. The former data are comparable to those registered for related white light NHC emitters of Pt(II) with dual emissions in PMMA films.[59] Despite their relatively low QY, the photometric and colorimetric parameters of the white light emitted are fairly close to the values reported for single-doped WOLEDs based on square-planar Pt(II) complexes (Table S5).[19−21,60,61] Hence, compound **7B** can provide white light emissions in the neutral range with correlated color temperatures (CCT) ranging from 3691 to 5106 K and excellent color rendering index (CRI) values of 90−75. Also, it is worth noting that solid-state emissions of **8A** and **7B** display CIE coordinates along the Planckian locus (|Duv| < 0.006) that strictly comply with the stipulated values for indoor solid-state illumination.[62−64]

CONCLUSIONS

A new cycloplatinated NHC complex was successfully prepared using our stepwise procedure and the organic synthons: ethyl-4-bromobenzoate and benzimidazole. Ionic, $[Pt(C\hat{}C^{*A/B})(P\hat{}P)]PF_6$, and neutral, $[Pt(C\hat{}C^{*A/B})(S\hat{}S)]$, compounds with the presence of two chelate ligands in the molecule, $C\hat{}C^{*A/B}$ and P^P (dpfppe, dcypm) or S^S (dmdtc, pdtc), were synthesized and fully characterized. Their structural and spectroscopical features were mainly determined by the cyclometalated $C\hat{}C^{*A/B}$ ligand; nonetheless, the nature of the ancillary ligand (P^P or S^S) was also a shaping factor. A larger π system in the benzimidazole derivatives (**A**) sustains π-stackings between adjacent molecules in the crystal structures of **6A** and **7A** and causes a downfield shift of the ^{195}Pt NMR signals when compared to those of the **B** ones, indicating a strong EW effect. Also, the benzimidazole fragment results to push their absorptions and emissions to lower energies in relation to the imidazole ones (**B**). Regarding the ancillary ligands, the emissions of the P^P derivatives show high-energy vibronic bands with those of the dpfppe derivatives being shifted to higher energies with respect to the dcypm ones. All P^P-derivatives are very good blue (**B**) and cyan (**A**) emitters in PMMA films (5 wt %) with photoluminescence quantum yield values reaching up to ∼90%. However, the absorptions and emissions of the S^S counterparts do not change with the different dithiocarbamates. In solid-state and in doped PMMA films, the high-energy vibronic band that arises from ^{3}ILCT/^{3}MLCT excited states is accompanied by an additional low-energy structureless band. This is attributed to the $^3\pi\pi^*$ transitions originated from π-stacked aggregates as a result of using less bulky ancillary ligands (S^S). Thus, white light emission can be obtained rendering low QY but CCT, CRI, and Duv values within the stipulated margins for general light applications.

EXPERIMENTAL SECTION

Synthesis of $[Pt(C\hat{}C^{*A})(dpfppe)]PF_6$ (5A). Bis-(dipentafluorophenylphosphino)ethane (126.3 mg, 0.165 mmol) and KPF_6 (30.9 mg, 0.165 mmol) were added to a suspension of **4A** (80 mg, 0.082 mmol) in 25 mL of acetone, and the mixture was stirred at rt for 2 h. Then the solvent was evaporated to dryness under reduced pressure, and the residue was treated with CH_2Cl_2 (40 mL). After filtering through Celite, the solution was evaporated to dryness. Addition of diethyl ether (10 mL) to the residue rendered **5A**. Yield: 163.3 mg, 73%. Anal. calcd for $C_{43}H_{19}F_{26}N_2O_2P_3Pt$: C, 37.49; H, 1.39; N, 2.03. Found: C, 37.87; H, 1.43; N, 2.10. ^{1}H plus ^{1}H{^{31}P} NMR (400 MHz, CD_2Cl_2, δ (ppm), J (Hz)): δ = 8.20 (d, 1H, $^3J_{H-H}$ = 8.2, H_{bzim}), 8.09 (dm, 1H, $^4J_{7-P}$ = 7.7, $^3J_{7-Pt}$ = 60.8, H_7), 8.00 (dd, 1H, $^3J_{9-10}$ = 8.3, $^4J_{9-7}$ = 1.5, H_9), 7.91 (dd, 1H, $^3J_{10-9}$ = 8.3, $^5J_{10-P}$ = 2.9, H_{10}), 7.72−7.55 (m, 3H, H_{bzim}), 4.30 (q, 2H, $^3J_{H-H}$ = 7.0, CH_2, OEt), 3.84 (s, 3H, H_4), 3.01 (m, 4H, CH_2, P^P), 1.30 (t, 3H, CH_3, OEt). ^{13}C{^{1}H} NMR (101 MHz, CD_2Cl_2): δ = 180.0 (C_1), 166.1 (COOEt), 152.4 (C_5), 149.6, 147.1, 144.3, and 140.2 (m, C_6F_5, P^P), 139.6 (C_7), 137.6 (m, C_6F_5, P^P), 130.6 (s, C_9), 128.0 and 126.8 (s, C_{bzim}), 113.4, 113.3, and 113.0 (s, C_{bzim}, and C_{10}), 61.9 (s, CH_2, OEt), 37.3 (s, C_4), 30.3 (m, CH_2, P^P), 29.2 (m, CH_2, P^P), 14.5 (s, CH_3, OEt). ^{31}P{^{1}H} NMR (162 MHz, CD_2Cl_2): δ = 14.4 (s, $^1J_{P-Pt}$ = 2784, P *trans* C_1), 6.0 (s, $^1J_{P-Pt}$ = 1774, P *trans* C_6). ^{19}F{^{1}H} NMR (377 MHz, CD_2Cl_2): δ = −74.4 (d, $^1J_{P-F}$ = 708.4, PF_6^-), −125.7 (s, br, 4F, F*o*), −127.2 (s, br, 4F, F*o*), −141.5 (t, 2F, $^3J_{Fp-Fm}$ = 20.0, F*p*), −142.2 (t, 2F, $^3J_{Fp-Fm}$ = 19.5, F*p*), −156.7 (dd, 4F, $^3J_{Fm-Fp}$ = $^3J_{Fm-Fo}$ = 19.5, F*m*), −157.2 (dd, 4F, $^3J_{Fm-Fp}$ = $^3J_{Fm-Fo}$ = 20.0, F*m*). ^{195}Pt{^{1}H} NMR (85.6 MHz, CD_2Cl_2): δ = −4718.0 (dd). IR (ATR, cm^{-1}): ν = 833 (s, PF_6), 556 (s, PF_6), 1711 (m, C═O). MS (MALDI+): m/z = 1232.8 $[C_{43}H_{19}F_{20}N_2O_2P_2Pt]^+$. Λ_M: 105.1 Ω^{-1} cm^2 mol^{-1}.

Synthesis of $[Pt(C\hat{}C^{*B})(dpfppe)]PF_6$ (5B). **5B** was prepared following the method for **5A**; dpfppe (131.94 mg, 0.174 mmol), KPF_6 (32.01 mg, 0.174 mmol), and **4B**[41] (80 mg, 0.087 mmol). **5B** (161.7 mg, 70%). Anal. calcd for $C_{39}H_{17}F_{26}N_2O_2P_3Pt$: C, 35.28; H, 1.29; N, 2.11. Found: C, 34.91; H, 1.25; N, 2.17. ^{1}H plus ^{1}H{^{31}P} NMR (400 MHz, CD_2Cl_2, δ (ppm), J (Hz)): δ = 7.98 (dm, 1H, $^4J_{7-P}$ = 8.0, $^3J_{7-Pt}$ = 59.4, H_7), 7.87 (dd, $^3J_{9-10}$ = 8.3, $^4J_{9-7}$ = 1.5, H_9), 7.55 (m, 1H, H_2), 7.26 (dd, $^3J_{10-9}$ = 8.3, $^5J_{10-P}$ = 2.7, H_{10}), 7.14 (m, 1H, H_3), 4.24 (q, $^3J_{H-H}$ = 7.2, 2H, CH_2, OEt), 3.56 (s, 3H, H_4), 3.05−2.75 (m, 4H, CH_2, P^P), 1.25 (t, $^3J_{H-H}$ = 7.2, 3H, CH_3, OEt). ^{13}C{^{1}H} NMR (101 MHz, CD_2Cl_2): δ = 169.8 (C_1), 165.9 (COOEt), 149.9 (C_5), 149.3, 146.7, 143.9, and 139.8 (m, C_6F_5, P^P), 138.3 (m, C_7), 137.2 (m, C_6F_5, P^P), 130.0 (s, C_9), 124.8 (s, C_3), 117.2 (s, C_2), 112.7 (s, C_{10}), 61.7 (s, CH_2, OEt), 39.2 (s, C_4), 30.2 (m, CH_2, P^P), 28.3 (m, CH_2, P^P), 14.5 (s, CH_3,OEt). ^{31}P{^{1}H} NMR (162 MHz, CD_2Cl_2): δ = 13.7 (s, $^1J_{P-Pt}$ = 2828, P *trans* C_1), 5.1 (s, $^1J_{P-Pt}$ = 1814, P *trans* C_6). ^{19}F{^{1}H} NMR (377 MHz, CD_2Cl_2): δ = −74.1 (d, $^1J_{P-F}$ = 709.5, PF_6^-), −125.7 (s, br, 4F, F*o*), −127.1 (s, br, 4F, F*o*), −141.3 (t, 2F, $^3J_{Fp-Fm}$ = 18.3, F*p*), −142.0 (t, 2F, $^3J_{Fp-Fm}$ = 19.9, F*p*), −156.5 (dd, 4F, $^3J_{Fm-Fp}$ = $^3J_{Fm-Fo}$ = 18.3, F*m*), −157.3 (dd, 4F, $^3J_{Fm-Fp}$ = $^3J_{Fm-Fo}$ = 19.9, F*m*). ^{195}Pt{^{1}H} NMR (85.6 MHz, CD_2Cl_2): δ = −4754.6 (dd). IR (ATR,cm^{-1}): ν= 833 (s, PF_6), 556 (s, PF_6), 1711 (m, C═O). MS (MALDI+): m/z = 1182.1 $[C_{39}H_{17}F_{20}N_2O_2P_2Pt]^+$. Λ_M: 116.0 Ω^{-1} cm^2 mol^{-1}.

Synthesis of $[Pt(C\hat{}C^{*A})(dcypm)]PF_6$ (6A). **6A** was prepared following the method for **5A**; dcypm (69.1 mg, 0.164 mmol), KPF_6 (30.9 mg, 0.164 mmol), and **4A** (80 mg, 0.082 mmol). **6A** (117.8 mg, 70%). Anal. calcd for $C_{42}H_{61}F_6N_2O_2P_3Pt$: C, 49.07; H, 5.98; N, 2.73. Found: C, 49.21; H, 5.73; N, 3.09. ^{1}H plus ^{1}H{^{31}P} NMR (400 MHz, CD_2Cl_2, δ (ppm), J (Hz)): δ = 8.25 (dm, 1H, $^4J_{7-P}$ = 8.0, $^3J_{7-Pt}$ = 62.9,H_7), 8.11 (d, 1H, $^3J_{H-H}$ = 8.1, H_{bzim}), 7.98 (dd, 1H, $^3J_{9-10}$ = 8.3, $^4J_{9-7}$ = 1.5, H_9), 7.82 (dd, 1H, $^3J_{10-9}$ = 8.3, $^5J_{10-P}$ = 2.3, H_{10}), 7.68 (dm, 1H, $^3J_{H-H}$ = 7.6, H_{bzim}), 7.58 (m, 2H, H_{bzim}), 4.37 (q, 2H, $^3J_{H-H}$ = 6.9, CH_2, OEt), 3.99 (s, 3H, H_4), 3.60 (t, 2H, $^2J_{H-P}$ = 9.8, CH_2, P^P), 2.50−1.27 (m, 47 H, CH, CH_2 (P^P), and CH_3 (OEt)). ^{13}C{^{1}H} NMR (101 MHz, CD_2Cl_2): δ = 183.1 (C_1), 165.9 (COOEt), 152.5 (C_5), 141.5 (m, C_7), 134.4 (C_{bzim}), 128.5 (s, C_9), 126.3 and 125.8 (s, C_{bzim}), 112.6, 112.5, and 112.3 (s, C_{bzim} and C_{10}), 60.6 (s, CH_2, OEt), 37.8 (s, C_4), 31.1−24.3 (m, Cy), 21.7 (t, $^1J_{C-P}$ = 26.2, CH_2, P^P), 13.8 (CH_3, OEt).^{31}P{^{1}H} NMR (162 MHz, CD_2Cl_2): δ = −22.0 (d, $^2J_{P-P}$ = 33.2, $^1J_{P-Pt}$ = 1455, P *trans* C_6), −24.4 (d, $^2J_{P-P}$ = 33.2, $^1J_{Pt-P}$ = 2273, P *trans* C_1). ^{195}Pt{^{1}H} NMR (85.6 MHz, CD_2Cl_2): δ = −4324.0 (dd). IR (ATR, cm^{-1}): ν = 834 (s, PF_6), 556 (s, PF_6), 1647 (m, C═O). MS (MALDI+): m/z = 882.1 $[C_{42}H_{61}N_2O_2P_2Pt]^+$. Λ_M: 121.9 Ω^{-1}cm^2 mol^{-1}.

Synthesis of $[Pt(C\hat{}C^{*B})(dcypm)]PF_6$ (6B). **6B** was prepared following the method for **5A**; dcypm (89.1 mg, 0.218 mmol), KPF_6 (40.1 mg, 0.218 mmol), and **4B** (100 mg, 0.109 mmol). **6B** (111.0 mg, 52%). Anal. calcd for $C_{38}H_{59}F_6N_2O_2P_3Pt$: C, 46.67; H, 6.08; N, 2.86. Found: C, 46.50; H, 5.94; N, 2.99. ^{1}H plus ^{1}H{^{31}P} NMR (400 MHz, CD_2Cl_2, δ (ppm), J (Hz)): δ= 8.17 (dm, 1H, $^4J_{7-P}$ = 7.4, $^3J_{7-Pt}$ =

https://dx.doi.org/10.1021/acs.organomet.0c00510
Organometallics XXXX, XXX, XXX−XXX

61.3, H_7), 7.86 (d, $^3J_{9-10}$ = 8.1, H_9), 7.45 (s, br, 1H, H_2), 7.22 (dd, 1H,$^3J_{10-9}$ = 8.1, $^5J_{10\text{-}P}$= 2.2, H_{10}), 7.19 (s, 1H, H_3), 4.34 (q, $^3J_{H-H}$ = 7.1, 2H, CH_2, OEt), 3.79 (s, 3H, H_4), 3.53 (t, 2H, $^2J_{H-P}$ = 9.6, CH_2, P^P), 2.4−1.2 (m, 47 H, CH, CH_2 (P^P), and CH_3 (OEt)). $^{13}C\{^1H\}$ NMR (101 MHz, CD_2Cl_2): δ = 174.1 (C_1), 166.3 (COOEt), 151.7 (C_5), 141.8 (m, C_7), 128.6 (s, C_9), 123.4 (s, C_3), 116.6 (s, C_2), 111.3 (s, C_{10}), 61.1 (s, CH_2, OEt), 39.6 (s, C_4), 36.8−26.0 (m, Cy), 23.2 (t, $^1J_{C-P}$ = 26.1, CH_2, P^P), 14.7 (s, CH_3, OEt). $^{31}P\{H\}$ NMR (162 MHz, CD_2Cl_2): δ = −23.1 (d, $^2J_{P-P}$ = 36, $^1J_{P-Pt}$ = 1500, P *trans* C_6), −25.8 (d, $^2J_{P-P}$ = 36, $^1J_{P-Pt}$ = 2288, P *trans* C_1). $^{195}Pt\{^1H\}$ NMR (85.6 MHz, CD_2Cl_2): δ = −4370.3(dd). IR (ATR, cm^{-1}): ν = 832 (s, PF_6), 556 (s, PF_6), 1644 (m, C═O). MS (MALDI+): m/z = 832.4 $[C_{38}H_{59}N_2O_2P_2Pt]^+$. Λ_M: 110.99 $\Omega^{-1}cm^2$ mol^{-1}.

Synthesis of [Pt(C^C*^{A})(dmdtc)] (7A). $AgPF_6$ (56.9 mg, 0.225 mmol) was added to a suspension of **4A** (109.1 mg, 0.113 mmol) in 40 mL of CH_3CN in a flask protected from the light, and the mixture was stirred for 5 h at rt. Then, the suspension was filtered through Celite, and the solution was concentrated to half of the original volume. Na(dmdtc) (32.2 mg, 0.225 mmol) was added to the resulting solution and left to react for 30 min. Then, the solvent was evaporated to dryness, and MeOH (20 mL) was added to the residue. The resulting solid was filtered and washed with MeOH (2 × 5 mL) and recrystallized from CH_2Cl_2/MeOH to give **7A** as a yellow solid. Yield: 61.1 mg, 46%. Anal. calcd for $C_{20}H_{21}N_3O_2PtS_2$: C, 40.40; H, 3.56; N, 7.07. Found: C, 40.08; H, 3.41; N, 7.04. ^1H NMR (400 MHz, CD_2Cl_2, δ (ppm), J (Hz)): δ = 8.06 (d, 1H, $^3J_{H-H}$= 7.9, H_{bzim}), 7.98 (d, $^4J_{7-9}$ = 1.2, $^3J_{7\text{-}Pt}$ = 71.4, 1H, H_7), 7.94 (dd, 1H, $^3J_{9-10}$ = 8.2, $^4J_{9-7}$ = 1.2, H_9), 7.69 (d, 1H, $^3J_{10-9}$ = 8.2, H_{10}), 7.48 (m, 3H, H_{bzim}), 4.39 (q, 2H, $^3J_{H-H}$= 7.2, CH_2,OEt), 3.93 (s, 3H, H_4), 3.43 (s, 6H, CH_3, dmtc), 1.43 (t, 3H, CH_3, OEt). $^{13}C\{^1H\}$NMR (101 MHz, CD_2Cl_2): δ = 210.9 (s, dmdtc), 172.7 (s, C_1), 135.4 (s, C_7), 126.8 (s, C_9), 125.1 and 124.0 (s, C_{bzim}), 112.0, 112.6, and 111.8 (s,C_{bzim} and C_{10}), 60.6 (s, CH_2,OEt), 39.8 (s, CH_3, dmdtc), 39.1 (s, CH_3, dmdtc), 34.0 (s, C_4), 14.5 (s, CH_3, OEt).$^{195}Pt\{^1H\}$ NMR (85.6 MHz, CD_2Cl_2): δ = −4082.2 (s). IR (ATR, cm^{-1}): ν = 1695 (s, C═O), 1539 (s, C−N), 949 (s, C−S), 364 (s,Pt−S). MS (MALDI+): m/z = 595.0 $[C_{20}H_{21}N_3O_2PtS_2]^+$.

Synthesis of [Pt(C^C*^{B})(dmdtc)] (7B). **7B** was obtained as a yellow solid following the method for **7A** but starting from **4B** (120 mg, 0.131 mmol), $AgPF_6$ (66.0 mg, 0.261 mmol), and Na(dmdtc) (37.7 mg, 0.261 mmol). Yield: 45.8 mg, 52%. Anal. calcd for $C_{16}H_{19}N_3O_2PtS_2$: C, 35.29; H, 3.52; N, 7.72. Found: C, 34.82; H, 3.33; N, 7.57. ^1H NMR (300 MHz, CD_2Cl_2, δ (ppm), J (Hz)): δ= 7.89 (d, 1H, $^3J_{7\text{-}Pt}$ = 69.3, $^4J_{7-9}$ = 1.8, H_7), 7.80 (dd, 1H, $^3J_{9-10}$ = 8.1, $^4J_{9-7}$ = 1.8, H_9), 7.33 (d, 1H, $^3J_{3-2}$ = 2.1, H_2), 7.10 (d, 1H, $^3J_{10-9}$= 8.1, H_{10}), 6.92 (d, 1H, $^3J_{3-2}$ = 2.0, $^4J_{3\text{-}Pt}$ = 11.4, H_3), 4.47 (q, 2H, $^3J_{H-H}$ = 6.95, CH_2, OEt), 3.75 (s, 3H, H_4), 3.40 (s, 3H, CH_3, dmdtc), 3.39 (s, 3H, CH_3, dmdtc), 1.37 (t, 3H, $^3J_{H-H}$ = 6.95, CH_3, OEt). $^{13}C\{^1H\}$ NMR (75 MHz, CD_2Cl_2): δ = 212.3 (s, dmdtc), 163.4 (s,C_1), 135.7 (s, C_7), 126.4 (s, C_9), 121.5 (s, C_3), 114.8 (s, C_2), 110.5 (s, C_{10}), 61.1 (s, CH_2), 40.0 (s, CH_3, dmdtc), 39.1 (s, CH_3, dmdtc), 37.0 (s, C_4), 14.8 (s, CH_3, OEt).$^{195}Pt\{^1H\}$NMR (85.6 MHz, CD_2Cl_2): δ = −4169.5(s). IR (ATR, cm^{-1}): ν = 1699 (s, C═O), 1541 (s, C−N), 956 (s, C−S), 371 (s, Pt−S). MS (MALDI+): m/z = 544.0 $[C_{16}H_{19}N_3O_2PtS_2]^+$.

Synthesis of [Pt(C^C*^{A})(pdtc)] (8A). **8A** was obtained as a yellow solid following the method for **7A** but using **4A** (80.0 mg, 0.082 mmol), $AgPF_6$ (41.7 mg, 0.165 mmol), and NH_4(pdtc) (27.1 mg, 0.165 mmol). Yield = 89.9 mg, 87.9%. Anal. calcd for $C_{22}H_{23}N_3O_2PtS_2$: C, 42.57; H, 3.74; N, 6.77. Found: C, 42.36; H, 3.36; N, 6.45. ^1H NMR (400 MHz, CD_2Cl_2, δ (ppm), J (Hz)): δ = 8.03 (d, 1H, $^3J_{H-H}$= 7.6, H_{bzim}), 7.94 (s, 1H, $^3J_{7\text{-}Pt}$ = 71.6, H_7), 7.90 (d, 1H, $^3J_{9-10}$ = 8.3, H_9), 7.66 (d, 1H, $^3J_{10\text{-}9}$= 8.3, H_{10}), 7.45 (m, 3H, H_{bzim}), 4.35 (q, 2H, $^3J_{H-H}$ = 6.9, CH_2, OEt), 3.89 (m, 7H, H_4 and N−CH_2, pdtc), 2.08 (m, 4H, CH_2, pdtc), 1.39 (t, 3H, $^3J_{H-H}$ = 6.9, CH_3, OEt). $^{13}C\{^1H\}$ NMR (101 MHz, CD_2Cl_2): δ = 171.2 (s, C_1), 166.4 (s, COOEt), 151.5 (s, C_5), 135.4 (s, C_7), 126.1 (s, C_9), 124.5 and 123.5 (s, C_{bzim}), 111.4, 111.3, and 111.2 (s, C_{bzim} and C_{10}), 60.4 (s, CH_2, OEt), 50.2 and 49.8 (s, CH_2−N, pdtc), 33.7 (s, C_4), 24.6 and 24.5 (s, CH_2, pdtc), 14.5 (CH_3, OEt).$^{195}Pt\{^1H\}$ NMR (85.6 MHz, CD_2Cl_2): δ = −4021.1 (s). IR (ATR, cm^{-1}): ν = 1690 (s, C═O), 1509 (s, C−N), 941 (s, C−S), 345 (s, Pt−S). MS (MALDI+): m/z = 621.0 $[C_{22}H_{23}N_3O_2PtS_2]^+$.

Synthesis of [Pt(C^C*^{B})(pdtc)] (8B). **8B** was obtained as a yellow solid following the method for **7A** but using **4B** (80.0 mg, 0.087 mmol), $AgPF_6$ (44.0 mg, 0.174 mmol), and NH_4(pdtc) (28.6 mg, 0.174 mmol). Yield = 53.0 mg, 56.9%. Anal. calcd for $C_{18}H_{21}N_3O_2PtS_2$: C, 37.89; H, 3.71; N, 7.36. Found: C, 37.53; H, 3.76; N, 7.01. ^1H NMR (400 MHz, CD_2Cl_2, δ (ppm), J (Hz)): δ= 7.87 (s, 1H, $^3J_{7\text{-}Pt}$ = 69.6, H_7), 7.79 (d, 1H, $^4J_{9-10}$ = 8.1, H_9), 7.33 (s, 1H, H_2), 7.10 (d, 1H, $^4J_{9-10}$ = 8.1, $^4J_{10\text{-}Pt}$ = 14.4, H_{10}), 6.92 (s, 1H, $^4J_{3\text{-}Pt}$ = 11.2, H_3), 4.32 (q, 2H, $^3J_{H-H}$ = 7.1, CH_2, OEt), 3.88 (m, 4H, CH_2, CH_2−N, pdtc), 3.7 (s, 3H, H_4), 2.08 (m, 4H, CH_2, pdtc), 1.41 (t, 3H, CH_3, OEt). $^{13}C\{^1H\}$ NMR (101 MHz, CD_2Cl_2): δ = 166.9 (s, COOEt), 162.7 (s, C_1), 151 (s, C_5), 135.6 (s, C_7), 126.3 (s, C_9), 121.4 (s, C_3), 114.7 (s, C_2), 110.5 (s, C_{10}), 61.0 (s, CH_2, OEt), 50.3 and 50.0 (s, CH_2−N, pdtc), 37.1 (s, C_4), 25.1 and 25.0 (s, CH_2, pdtc), 14.8 (s, CH_3, OEt).$^{195}Pt\{^1H\}$NMR (85.6 MHz, CD_2Cl_2): δ = −4107.7(s). IR (ATR, cm^{-1}): ν = 1700 (s, C═O), 1506 (s, C−N), 956 (s, C−S), 345 (s, Pt−S). MS (MALDI+): m/z = 569.9 $[C_{18}H_{21}N_3O_2PtS_2]^+$.

■ ASSOCIATED CONTENT

Supporting Information

The Supporting Information is available free of charge at https://pubs.acs.org/doi/10.1021/acs.organomet.0c00510.

Cartesian coordinates (XYZ)

General procedures, crystallographic and computational details; synthesis and characterization of compounds **1A**−**4A**; NMR spectra; X-ray diffraction data and structures; theoretical calculations; UV−vis, and emission spectra (PDF)

Accession Codes

CCDC 2011714−2011716 contain the supplementary crystallographic data for this paper. These data can be obtained free of charge via www.ccdc.cam.ac.uk/data_request/cif, or by emailing data_request@ccdc.cam.ac.uk, or by contacting The Cambridge Crystallographic Data Centre, 12 Union Road, Cambridge CB2 1EZ, UK; fax: +44 1223 336033.

■ AUTHOR INFORMATION

Corresponding Authors

Sara Fuertes − *Departamento de Química Inorgánica, Facultad de Ciencias, Instituto de Síntesis Química y Catálisis Homogénea (ISQCH), CSIC - Universidad de Zaragoza, 50009 Zaragoza, Spain;* orcid.org/0000-0003-1812-3175; Email: sfuertes@unizar.es

Violeta Sicilia − *Departamento de Química Inorgánica, Escuela de Ingeniería y Arquitectura de Zaragoza, Instituto de Síntesis Química y Catálisis Homogénea (ISQCH), CSIC - Universidad de Zaragoza, 50018 Zaragoza, Spain;* orcid.org/0000-0002-0257-0483; Email: sicilia@unizar.es

Authors

Sara Jaime − *Departamento de Química Inorgánica, Facultad de Ciencias, Instituto de Síntesis Química y Catálisis Homogénea (ISQCH), CSIC - Universidad de Zaragoza, 50009 Zaragoza, Spain*

Lorenzo Arnal − *Departamento de Química Inorgánica, Facultad de Ciencias, Instituto de Síntesis Química y Catálisis Homogénea (ISQCH), CSIC - Universidad de Zaragoza, 50009 Zaragoza, Spain;* orcid.org/0000-0002-0283-9307

Complete contact information is available at: https://pubs.acs.org/10.1021/acs.organomet.0c00510

https://dx.doi.org/10.1021/acs.organomet.0c00510
Organometallics XXXX, XXX, XXX−XXX

Notes

The authors declare no competing financial interest.

■ ACKNOWLEDGMENTS

This work was supported by the Spanish Ministerio de Ciencia, Innovación y Universidades/FEDER (project PGC2018-094749−B-I00), the Gobierno de Aragón (Grupo E17_20R), and Feder 2014-2020 (Construyendo Europa desde Aragón). S.F. thanks the Spanish National Research Council for grant no. 2018801070-PIE-147. L.A. acknowledges the support of a grant from the Gobierno de Aragon. The authors thank the Centro de Supercomputación de Galicia (CESGA) for generous allocation of computational resources.

■ REFERENCES

(1) Coppo, P. The day lighting became organic. *Photochemistry* **2009**, *37*, 393−404.
(2) *2011 Critical Materials Strategy*, DOE/PI-0009. U. S. Department of Energy: Washington, DC, 2012.
(3) Misra, A.; Kumar, P.; Kamalasanan, M. N.; Chandra, S. White Organic LEDs and their Recent Advancements. *Semicond. Sci. Technol.* **2006**, *21*, R35−R47.
(4) Reineke, S.; Thomschke, M.; Lüssem, B.; Leo, K. White Organic Light-emitting Diodes: Status and Perspective. *Rev. Mod. Phys.* **2013**, *85*, 1245−1293.
(5) Wang, L. X.; Wong, W.-Y.; Lin, M.-F.; Wong, W.-K.; Cheah, K.-W.; Tam, H.-L.; Chen, C. H. Novel Host Materials for Single-component White Organic Light-Emitting Diodes based on 9-naphthylanthracene derivatives. *J. Mater. Chem.* **2008**, *18*, 4529−4536.
(6) Coppo, P.; Duati, M.; Kozhevnikov, V. N.; Hofstraat, J. W.; De Cola, L. White-Light Emission from an Assembly Comprising Luminescent Iridium and Europium Complexes. *Angew. Chem., Int. Ed.* **2005**, *44*, 1806−1810.
(7) Bolink, H. J.; De Angelis, F.; Baranoff, E.; Klein, C.; Fantacci, S.; Coronado, E.; Sessolo, M.; Kalyanasundaram, K.; Gratzel, M.; Nazeeruddin, M. K. White-Light Phosphorescence Emission from a Single Molecule: Application to OLED. *Chem. Commun.* **2009**, 4672−4674.
(8) He, K. Q.; Wang, X. D.; Yu, J. T.; Jiang, H. G.; Xie, G. S.; Tan, H.; Liu, Y.; Ma, D. G.; Wang, Y. F.; Zhu, W. G. Synthesis and Optoelectronic Properties of Novel Fluorene-Bridged Dinuclear Cyclometalated Iridium (III) Complex with A-D-A Framework in the Single-Emissive-Layer WOLEDs. *Org. Electron.* **2014**, *15*, 2942−2949.
(9) He, G.; Guo, D.; He, C.; Zhang, X.; Zhao, X. H.; Duan, C. A Color-Tunable Europium Complex Emitting Three Primary Colors and White Light. *Angew. Chem., Int. Ed.* **2009**, *48*, 6132−6135.
(10) Xie, M.; Han, C.; Zhang, J.; Xie, G.; Xu, H. White Electroluminescent Phosphine-Chelated Copper Iodide Nanoclusters. *Chem. Mater.* **2017**, *29*, 6606−6610.
(11) Li, X.; Liu, Y.; Luo, J.; Zhang, Z.; Shi, D.; Chen, Q.; Wang, Y. F.; He, J.; Li, J.; Lei, G.; Zhu, W. Synthesis and Optoelectronic Properties of a Heterobimetallic Pt(II)−Ir(III) Complex Used as a Single-Component Emitter in White PLEDs. *Dalton Trans.* **2012**, *41*, 2972−2978.
(12) Tsai, M.-L.; Liu, C.-Y.; Hsu, M.-A.; Chow, T. J. White Light Emission from Single Component Polymers Fabricated by Spin Coating. *Appl. Phys. Lett.* **2003**, *82*, 550−552.
(13) Cocchi, M.; Kalinowski, J.; Virgili, D.; Fattori, V.; Develay, S.; Williams, J. A. G. Single-Dopant Organic White Electrophosphorescent Diodes with Very High Efficiency and Its Reduced Current Density Roll-Off. *Appl. Phys. Lett.* **2007**, *90*, 163508.
(14) Wang, X.; Chang, Y. L.; Lu, J. S.; Zhang, T.; Lu, Z. H.; Wang, S. N. Bright Blue and White Electrophosphorescent Triarylboryl-Functionalized C ^N-Chelate Pt(II) Compounds: Impact of Intramolecular Hydrogen Bonds and Ancillary Ligands. *Adv. Funct. Mater.* **2014**, *24*, 1911−1927.
(15) Adamovich, V.; Brooks, J.; Tamayo, A.; Alexander, A. M.; Djurovich, P. I.; D'Andrade, B. W.; Adachi, C.; Forrest, S. R.; Thompson, M. E. High Efficiency Single Dopant White Electrophosphorescent Light Emitting Diodes. *New J. Chem.* **2002**, *26*, 1171−1178.
(16) D'Andrade, B. W.; Brooks, J.; Adamovich, V.; Thompson, M. E.; Forrest, S. R. White Light Emission Using Triplet Excimers in Electrophosphorescent Organic Light-Emitting Devices. *Adv. Mater.* **2002**, *14*, 1032−1036.
(17) Cocchi, M.; Kalinowski, J.; Murphy, L.; Williams, J. A. G.; Fattori, V. Mixing of Molecular Exciton and Excimer Phosphorescence to Tune Color and Efficiency of Organic LEDs. *Org. Electron.* **2010**, *11*, 388−396.
(18) Fleetham, T.; Ecton, J.; Wang, Z.; Bakken, N.; Li, J. H. Single-Doped White Organic Light-Emitting Device with an External Quantum Efficiency Over 20%. *Adv. Mater.* **2013**, *25*, 2573−2576. and references therein
(19) Fleetham, T.; Huang, L.; Li, J. Tetradentate Platinum Complexes for Efficient and Stable Excimer-Based White OLEDs. *Adv. Funct. Mater.* **2014**, *24*, 6066−6073.
(20) Li, G. J.; Fleetham, T.; Li, J. Efficient and Stable White Organic Light-Emitting Diodes Employing a Single Emitter. *Adv. Mater.* **2014**, *26*, 2931−2936.
(21) Cheng, G.; Chow, P. K.; Kui, S. C. F.; Kwok, C. C.; Che, C. M. High-Efficiency Polymer Light-Emitting Devices with Robust Phosphorescent Platinum(II) Emitters Containing Tetradentate Dianionic O^N^C^N Ligands. *Adv. Mater.* **2013**, *25*, 6765−6770.
(22) Kui, S. C. F.; Chow, P. K.; Tong, G. S. M.; Lai, S. L.; Cheng, G.; Kwok, C. C.; Low, K. H.; Ko, M. Y.; Che, C. M. Robust Phosphorescent Platinum(II) Complexes Containing Tetradentate O^N^C^N Ligands: Excimeric Excited State and Application in Organic White-Light-Emitting Diodes. *Chem. - Eur. J.* **2013**, *19*, 69−73.
(23) Bhansali, U. S.; Jia, H.; Oswald, I. W. H.; Omary, M. A.; Gnade, B. E. High Efficiency Warm-White Organic Light Emitting Diodes From A Single Emitter in Graded-Doping Device Architecture. *Appl. Phys. Lett.* **2012**, *100*, 183305.
(24) Zhou, G.; Wang, Q.; Ho, C.-L.; Wong, W.-Y.; Ma, D.; Wang, L. Duplicating "Sunlight" from Simple Woleds for Lighting Applications. *Chem. Commun.* **2009**, 3574−3576.
(25) Tan, G.; Chen, S.; Siu, C.-H.; Langlois, A.; Qiu, Y.; Fan, H.; Ho, C.-L.; Harvey, P. D.; Lo, Y. H.; Liu, L.; Wong, W.-Y. Platinum(II) Cyclometallates Featuring Broad Emission Bands and their Applications in Color-Tunable OLEDs and High Color-Rendering WOLEDs. *J. Mater. Chem. C* **2016**, *4*, 6016−6026.
(26) Zhou, G. J.; Wang, Q.; Wang, X. Z.; Ho, C. L.; Wong, W. Y.; Ma, D. G.; Wang, L. X.; Lin, Z. Y. Metallophosphors of Platinum with Distinct Main-Group Elements: a Versatile Approach towards Color Tuning and White-Light Emission with Superior Efficiency/Color Quality/Brightness Trade-Offs. *J. Mater. Chem.* **2010**, *20*, 7472−7484.
(27) Li, K.; Cheng, G.; Ma, C.; Guan, X.; Kwok, W.-M.; Chen, Y.; Lu, W.; Che, C.-M. Light-Emitting Platinum(II) Complexes Supported by Tetradentate Dianionic Bis(N-Heterocyclic Carbene) Ligands: Towards Robust Blue Electrophosphors. *Chem. Sci.* **2013**, *4*, 2630−2644.
(28) Unger, Y.; Meyer, D.; Molt, O.; Schildknecht, C.; Münster, I.; Wagenblast, G.; Strassner, T. Green−Blue Emitters: NHC-Based Cyclometalated [Pt(C^C*)(acac)] Complexes. *Angew. Chem., Int. Ed.* **2010**, *49*, 10214−10216.
(29) Strassner, T. Phosphorescent Platinum(II) Complexes with C^C* Cyclometalated NHC Ligands. *Acc. Chem. Res.* **2016**, *49*, 2680−2689.
(30) Elie, M.; Renaud, J. L.; Gaillard, S. N-Heterocyclic Carbene Transition Metal Complexes in Light Emitting Devices. *Polyhedron* **2018**, *140*, 158−168.
(31) Zou, T.; Hung, F. F.; Yang, C.; Che, C. M. Strongly Phosphorescent Transition-Metal Complexes with N-Heterocyclic Carbene Ligands as Cellular Probes. In *Luminescent and Photoactive Transition Metal Complexes as Biomolecular Probes and Cellular*

https://dx.doi.org/10.1021/acs.organomet.0c00510
Organometallics XXXX, XXX, XXX−XXX

Reagents; Lo, K. K. W., Ed.; Springer-Verlag: Berlin, 2015; Vol. *165*, pp 181−203.
(32) Liu, W. K.; Gust, R. Update on Metal N-heterocyclic Carbene Complexes as Potential Anti-Tumor Metallodrugs. *Coord. Chem. Rev.* **2016**, *329*, 191−213.
(33) Prokhorov, A. M.; Hofbeck, T.; Czerwieniec, R.; Suleymanova, A. F.; Kozhevnikov, D. N.; Yersin, H. Brightly Luminescent Pt(II) Pincer Complexes with a Sterically Demanding Carboranyl-Phenylpyridine Ligand: A New Material Class for Diverse Optoelectronic Applications. *J. Am. Chem. Soc.* **2014**, *136*, 9637−9642.
(34) Li, G.; Zhao, X. H.; Fleetham, T.; Chen, Q.; Zhan, F.; Zheng, J.; Yang, Y.-F.; Lou, W.; Yang, Y.; Fang, K.; Shao, Z.; Zhang, Q.-C.; She, Y. Tetradentate Platinum(II) Complexes for Highly Efficient Phosphorescent Emitters and Sky Blue OLEDs. *Chem. Mater.* **2020**, *32*, 537−548.
(35) Yersin, H.; Rausch, A. F.; Czerwieniec, R.; Hofbeck, T.; Fischer, T. The Triplet State of Organo-Transition Metal Compounds. Triplet Harvesting and Singlet Harvesting for Efficient OLEDs. *Coord. Chem. Rev.* **2011**, *255*, 2622−2652.
(36) Sicilia, V.; Arnal, L.; Chueca, A. J.; Fuertes, S.; Babaei, A.; Igual Munoz, A. M.; Sessolo, M.; Bolink, H. J. Highly Photoluminescent Blue Ionic Platinum-Based Emitters. *Inorg. Chem.* **2020**, *59*, 1145−1152.
(37) Fuertes, S.; Chueca, A. J.; Martín, A.; Sicilia, V. New NHC Cycloplatinated Compounds. Significance of the Cyclometalated Group on the Electronic and Emitting Properties of Biscyanide Compounds. *J. Organomet. Chem.* **2019**, *889*, 53−61.
(38) Sicilia, V.; Fuertes, S.; Chueca, A. J.; Arnal, L.; Martín, A.; Perálvarez, M.; Botta, C.; Giovanella, U. Highly Efficient Platinum-Based Emitters for Warm White Light Emitting Diodes. *J. Mater. Chem. C* **2019**, *7*, 4509−4516.
(39) Arnal, L.; Fuertes, S.; Martin, A.; Sicilia, V. The Use of Cyclometalated NHCs and Pyrazoles for the Development of Fully Efficient Blue Pt-II Emitters and Pt/Ag Clusters. *Chem. - Eur. J.* **2018**, *24*, 9377−9384.
(40) Fuertes, S.; Chueca, A. J.; Arnal, L.; Martín, A.; Giovanella, U.; Botta, C.; Sicilia, V. Heteroleptic Cycloplatinated N-heterocyclic Carbene Complexes: A New Approach to Highly Efficient Blue-Light Emitters. *Inorg. Chem.* **2017**, *56*, 4829−4839.
(41) Fuertes, S.; Chueca, A. J.; Perálvarez, M.; Borja, P.; Torrell, M.; Carreras, J.; Sicilia, V. White Light Emission from Planar Remote Phosphor Based on NHC Cycloplatinated Complexes. *ACS Appl. Mater. Interfaces* **2016**, *8*, 16160−16169.
(42) Fuertes, S.; García, H.; Perálvarez, M.; Hertog, W.; Carreras, J.; Sicilia, V. Stepwise Strategy to Cyclometallated PtII Complexes with *N*-Heterocyclic Carbene Ligands: A Luminescence Study on New *β*-Diketonate Complexes. *Chem. - Eur. J.* **2015**, *21*, 1620−1631.
(43) Fuertes, S.; Chueca, A. J.; Sicilia, V. Exploring the Transphobia Effect on Heteroleptic NHC Cycloplatinated Complexes. *Inorg. Chem.* **2015**, *54*, 9885−9895.
(44) Fuertes, S.; Chueca, A. J.; Martín, A.; Sicilia, V. Pt_2Tl Building Blocks for Two-Dimensional Extended Solids: Synthesis, Crystal Structures, and Luminescence. *Cryst. Growth Des.* **2017**, *17*, 4336−4346.
(45) Casas, J. M.; Fornies, J.; Fuertes, S.; Martin, A.; Sicilia, V. New Mono- and Polynuclear Alkynyl Complexes Containing Phenylacetylide as Terminal or Bridging Ligand. X-Ray Structures of the Compounds NBu_4 $Pt(CH_2C_6H_4P(o\text{-}tolyl)_2\text{-}\kappa$ C,P)(C CPh)$_2$, $Pt(CH_2C_6H_4P(o\text{-}tolyl)_2\text{-}\kappa$ C,P)(C CPh)(CO), $\{Pt(CH_2C_6H_4P(o\text{-}tolyl)_2\text{-}\kappa$ C,P)(μ-CCPh)$\}_2$, and $\{Pt(CH_2C_6H_4P(o\text{-}tolyl)_2\text{-}\kappa$ C,P)(C CPh)$_2$Cu$\}_2$. *Organometallics* **2007**, *26*, 1674−1685.
(46) Vicente, J.; Abad, J. A.; Martinez-Viviente, E.; Jones, P. G. Study of the Reactivity of 2-Acetyl-, 2-Cyano-, 2-Formyl-, and 2-Vinylphenyl Palladium(II) Complexes. Mono- and Triinsertion of an Isocyanide into the Pd-C Bond. A 2-Cyanophenyl Palladium Complex as a Ligand. *Organometallics* **2002**, *21*, 4454−4467.
(47) Maidich, L.; Zuri, G.; Stoccoro, S.; Cinellu, M. A.; Zucca, A. Assembly of Symmetrical and Unsymmetrical Platinum(II) Rollover Complexes with Bidentate Phosphine Ligands. *Dalton Trans.* **2014**, *43*, 14806−14815.
(48) Garrou, P. E. Delta-R Ring Contributions to P-31 Nmr Parameters of Transition-Metal-Phosphorus Chelate Complexes. *Chem. Rev.* **1981**, *81*, 229−266.
(49) Coucouvanis, D. In *Progress in Inorganic Chemistry*; Lippard, S. J., Ed.; John Wiley and Sons: New York, 1979; p 424.
(50) Exarchos, G.; Robinson, S. D.; Steed, J. W. The Synthesis of New Bimetallic Complex Salts by Halide/Sulfur Chelate Cross Transfer: X-Ray Crystal Structures of the Salts $Ni(S_2CNEt_2)(dppe)_2$ $HgBr_4$, $Pt(S_2CNEt_2)(dppe)_2$ $CdCl_4$, $Co(S_2CNEt_2)_2(dppe)_2$ Cl_3ZnO: $(Ph)_2PCH_2CH_2P(Ph)_2$: $OZnCl_3$ and $Pd((S_2CNBu_2)\text{-}Bu\text{-}n)(bipy)_2$ $CdCl_4$. *Polyhedron* **2001**, *20*, 2951−2963.
(51) Fornies, J.; Sicilia, V.; Casas, J. M.; Martin, A.; Lopez, J. A.; Larraz, C.; Borja, P.; Ovejero, C. Pt-Ag Clusters and Their Neutral Mononuclear Pt(II) Starting Complexes: Structural and Luminescence Studies. *Dalton Trans.* **2011**, *40*, 2898−2912.
(52) Fornies, J.; Martin, A.; Sicilia, V.; Villarroya, P. Reactivity of $[M(C\text{^}P)(S_2CNMe_2)]$ [M = Pt, Pd; C^P= $CH_2\text{-}C_6H_4\text{-}P(o\text{-}tolyl)_2$-kC,P] toward mercury(II) carboxylates. X-ray molecular structures of $Pt(C\text{^}P)(S_2CNMe_2)(O_2CCF_3)Hg(O_2CCF_3)$ and $Pd(S_2CNMe_2)\text{-}\{\mu\text{-}P(o\text{-}tolyl)_2\text{-}C_6H_4\text{-}CH_2\text{-}\}(\mu\text{-}O_2CCH_3)Hg(O_2CCH_3)$. *Organometallics* **2000**, *19*, 1107−1114.
(53) Tronnier, A.; Heinemeyer, U.; Metz, S.; Wagenblast, G.; Muenster, I.; Strassner, T. Heteroleptic Platinum(II) NHC Complexes with a C^C* Cyclometalated Ligand − Synthesis, Structure and Photophysics. *J. Mater. Chem. C* **2015**, *3*, 1680−1693.
(54) Fleetham, T.; Wang, Z. X.; Li, J. Efficient Deep Blue Electrophosphorescent Devices Based on Platinum(II) Bis(n-methyl-imidazolyl)benzene Chloride. *Org. Electron.* **2012**, *13*, 1430−1435.
(55) Hudson, Z. M.; Sun, C.; Helander, M. G.; Chang, Y. L.; Lu, Z. H.; Wang, S. N. Highly Efficient Blue Phosphorescence from Triarylboron-Functionalized Platinum(II) Complexes of N-Heterocyclic Carbenes. *J. Am. Chem. Soc.* **2012**, *134*, 13930−13933.
(56) Hang, X.-C.; Fleetham, T.; Turner, E.; Brooks, J.; Li, J. Highly Efficient Blue-Emitting Cyclometalated Platinum(II) Complexes by Judicious Molecular Design. *Angew. Chem., Int. Ed.* **2013**, *52*, 6753−6756.
(57) Li, G.; Wolfe, A.; Brooks, J.; Zhu, Z.-Q.; Li, J. Modifying Emission Spectral Bandwidth of Phosphorescent Platinum(II) Complexes Through Synthetic Control. *Inorg. Chem.* **2017**, *56*, 8244−8256.
(58) Bevilacqua, J. M.; Eisenberg, R. Synthesis and Characterization of Luminescent Square-Planar Platinum(II) Complexes Containing Dithiolate or Dithiocarbamate Ligands. *Inorg. Chem.* **1994**, *33*, 2913−2923.
(59) Bachmann, M.; Suter, D.; Blacque, O.; Venkatesan, K. Tunable and Efficient White Light Phosphorescent Emission Based on Single Component N-Heterocyclic Carbene Platinum(II) Complexes. *Inorg. Chem.* **2016**, *55*, 4733−4745.
(60) Cheng, G.; Kui, S. C. F.; Ang, W.-H.; Ko, M.-Y.; Chow, P.-K.; Kwong, C.-L.; Kwok, C.-C.; Ma, C.; Guan, X.; Low, K.-H.; Su, S.-J.; Che, C.-M. Structurally Robust Phosphorescent [Pt(O^N^C^N)] Emitters For High Performance Organic Light-Emitting Devices with Power Efficiency up to 126 Lm W^{-1} and External Quantum Efficiency Over 20%. *Chem. Sci.* **2014**, *5*, 4819−4830.
(61) Williams, E. L.; Haavisto, K.; Li, J.; Jabbour, G. E. Excimer-Based White Phosphorescent Organic Light Emitting Diodes with Nearly 100% Internal Quantum Efficiency. *Adv. Mater.* **2007**, *19*, 197−202.
(62) *ANSI C78.374-2015: Light-Emitting Diode Package Specification Sheet for General Illumination Applications*; NEMA: Arlington, VA, 2016.
(63) Erdem, T.; Demir, H. V. Color Science of Nanocrystal Quantum Dots for Lighting and Displays. *Nanophotonics* **2013**, *2*, 57−81.
(64) Gather, M. C.; Köhnen, A.; Meerholz, K. White Organic Light-Emitting Diodes. *Adv. Mater.* **2011**, *23*, 233−248.

https://dx.doi.org/10.1021/acs.organomet.0c00510
Organometallics XXXX, XXX, XXX−XXX